

# UNIVERSITY OF BIRMINGHAM

University of Birmingham  
Research at Birmingham

## Robust retrofitting design for rehabilitation of segmental tunnel linings

Zhang, Dong-ming; Zhai, Wu-zhou; Huang, Hong-wei; Chapman, David

DOI:

[10.1016/j.tust.2018.09.016](https://doi.org/10.1016/j.tust.2018.09.016)

License:

Creative Commons: Attribution-NonCommercial-NoDerivs (CC BY-NC-ND)

*Document Version*

Peer reviewed version

*Citation for published version (Harvard):*

Zhang, D, Zhai, W, Huang, H & Chapman, D 2019, 'Robust retrofitting design for rehabilitation of segmental tunnel linings: using the example of steel plates', *Tunnelling and Underground Space Technology*, vol. 83, pp. 231-242. <https://doi.org/10.1016/j.tust.2018.09.016>

[Link to publication on Research at Birmingham portal](#)

### **Publisher Rights Statement:**

Checked for eligibility: 23/10/2018

### **General rights**

Unless a licence is specified above, all rights (including copyright and moral rights) in this document are retained by the authors and/or the copyright holders. The express permission of the copyright holder must be obtained for any use of this material other than for purposes permitted by law.

- Users may freely distribute the URL that is used to identify this publication.
- Users may download and/or print one copy of the publication from the University of Birmingham research portal for the purpose of private study or non-commercial research.
- User may use extracts from the document in line with the concept of 'fair dealing' under the Copyright, Designs and Patents Act 1988 (?)
- Users may not further distribute the material nor use it for the purposes of commercial gain.

Where a licence is displayed above, please note the terms and conditions of the licence govern your use of this document.

When citing, please reference the published version.

### **Take down policy**

While the University of Birmingham exercises care and attention in making items available there are rare occasions when an item has been uploaded in error or has been deemed to be commercially or otherwise sensitive.

If you believe that this is the case for this document, please contact [UBIRA@lists.bham.ac.uk](mailto:UBIRA@lists.bham.ac.uk) providing details and we will remove access to the work immediately and investigate.

**Robust Retrofitting Design for Rehabilitation of Segmental Tunnel Linings:**

**Using the Example of Steel Plates**

Dong-ming Zhang<sup>a</sup>, Wu-zhou Zhai<sup>b</sup>, Hong-wei Huang<sup>c,\*</sup>, David Chapman<sup>d</sup>

<sup>a</sup> Assistant Professor, Key Laboratory of Geotechnical and Underground Engineering of Minister of Education and Department of Geotechnical Engineering, Tongji University, Shanghai, China. [09zhang@tongji.edu.cn](mailto:09zhang@tongji.edu.cn)

<sup>b</sup> Ph.D candidate, Key Laboratory of Geotechnical and Underground Engineering of Minister of Education and Department of Geotechnical Engineering, Tongji University, Shanghai, China. [zhaiwuzhou@tongji.edu.cn](mailto:zhaiwuzhou@tongji.edu.cn)

<sup>c</sup> Professor, Key Laboratory of Geotechnical and Underground Engineering of Minister of Education and Department of Geotechnical Engineering, Tongji University, Shanghai, China. [huanghw@tongji.edu.cn](mailto:huanghw@tongji.edu.cn)

<sup>d</sup> Professor, School of Civil Engineering, College of Engineering and Physical Sciences, University of Birmingham, Edgbaston, Birmingham, UK. [d.n.chapman@bham.ac.uk](mailto:d.n.chapman@bham.ac.uk)

17

18     **Robust Retrofitting Design for Rehabilitation of Segmental Tunnel Linings:**

19                     **Using the Example of Steel Plates**

20

21     **Abstract:** This paper presents a general framework for the robust retrofitting design  
22     for rehabilitation of segmental tunnel linings installed using shield tunnelling, and  
23     specifically using steel plates bonded to the lining as a typical example of such a  
24     rehabilitation design. A two-dimensional finite element model is established as part of  
25     the robust design which can simulate the deformational response of the steel plates  
26     reinforced segmental tunnel lining. The surrounding soil, the tunnel lining, the steel  
27     plates and the interactions between each of these are all properly simulated in this  
28     model and verified by full-scale test results. The change in horizontal convergence  
29     ( $\Delta D_{hs}$ ) subjected to environmental impact, such as unexpected placement of ground  
30     surface surcharge is measured to reflect the performance of segmental tunnel linings  
31     reinforced by steel plates. The standard deviation of the reinforced tunnel  
32     performance due to uncertainties in the soil conditions and the ground surface  
33     surcharge is derived to measure the design robustness. A robust rehabilitation design  
34     is then accomplished by varying the steel plates sizes (i.e. width and thickness) to  
35     maximize the design robustness and minimize the cost using a multi-objective  
36     algorithm, also considering the safety requirement constraints. The optimal designs  
37     are determined as a set of design points, namely a Pareto Front, which presents a  
38     trade-off relationship between the design objectives and is demonstrated as being

useful for decision making. Finally, the robust rehabilitation design method is applied to the retrofitting design of tunnel lining using steel plates in a real case study, and a comparison between the actual design and the design derived by the proposed method has been made to show its applicability and potentially significant advantages for designers, as the method allows consideration of both the highest robustness and the lowest cost simultaneously.

**Key words:** Robust design, segmental tunnel lining, steel plates, uncertainties, decision making

## **1. Introduction**

The worldwide long-term development of urban metro system has driven the wide use of shield tunneling in construction especially in soft ground. Hence, segmentally lined tunnels installed by shield tunnelling have been utilized for decades, for example London, Tokyo and Shanghai. However, as a typically prefabricated assembled concrete structure, a segmental tunnel lining is vulnerable to nearby disturbance especially in soft ground conditions such as those experienced in Shanghai. Large deformation in terms of transverse convergence and longitudinal settlement, and the associated severe structural defects such as leakage, concrete cracking and spalling have been detected in segmentally lined tunnels from on-site inspection and monitoring data (Shi and Li, 2015; Yuan et al., 2013). The structural health of segmental linings are likely to be adversely affected by nearby engineering activities and human-error related hazards. A typical example was reported by Huang et al. (2017) for a field case study involving an extreme surcharge being applied to a

running metro tunnel in Shanghai. Therefore effective rehabilitation treatments for distressed concrete segmental linings are of great importance, especially at this time of rapid development of shield tunnel construction.

There are several methods suitable for repairing and strengthening segmental tunnel linings, for example bonding fiber reinforced polymer (FRP) or steel plates to the inner surface of segmental concrete linings (Liu and Zhang, 2014; Kiriyaama et al., 2005), and grouting on either side of the tunnel at its spring line (Zhang et al., 2014). From these repair measures, bonding steel plates to an existing lining is often chosen as a permanent strengthening method. This rehabilitation approach using bonded steel plates can potentially enhance both the structural stiffness and the ultimate capacity (Kiriyaama et al., 2005). Furthermore, the construction operations associated with bonding steel plates can rely on standard machinery resulting in a fast and effective repair procedure. Hence, bonding the steel plates has been successfully adopted as a permanent rehabilitation method in many projects involving damaged segmental tunnel linings worldwide (Chang et al., 2001; Huang and Zhang, 2016).

Kiriyaama et al. (2005) presented an analytical analysis for the design of steel plate reinforcement for existing deformed tunnels utilizing a beam spring model. In the model, the steel plates are modelled as a circumferential beam, and a series of nonlinear springs with no tensile resistance are applied in the radial direction to simulate the interaction. Based on the practice of steel plate reinforcement frequently used in Shanghai, Zhao et al. (2015) conducted a full scale load test on a steel plate reinforced segmental lining ring. In their study, a simplified numerical model was

established to further investigate the mechanical and deformational behaviour of reinforced tunnel linings. Apart from these researchers providing insight into the structural response of the lining, other research has focused on the bonding behaviour and failure mode of epoxy bonded steel plate reinforcing concrete structures ([Ziraba et al., 1995](#); [Adhikary et al., 2002](#)). Previous literature on numerical simulations provide a basic understanding of the effectiveness of bonding steel plates on the disrupted tunnel structures. However, the model used previously simplified the behaviour of the surrounding soils by using soil springs based on Winkler's model ([Do, et al., 2015](#); [Zhang et al., 2017](#)). This simplification will further contribute to any discrepancy between the prediction and the field measurements, especially when the ground conditions are very uncertain in the context of soil properties. Furthermore, the design of steel plate rehabilitation mainly depends on the engineering experience. Hence, an appropriate design model for the rehabilitation of segmental tunnel linings that can be robust appropriate for the environmental uncertainty would be extremely welcome.

A robust design methodology was originally developed by [Taguchi & Wu \(1979\)](#) for improving the industrial product quality and manufacturability. Since then a great many studies have been conducted to understand this idea and make it applicable to other areas. The main idea behind a robust design is to make the system response insensitive to (robust against) hard-to-control disturbances (called noise factors) at a low cost ([Kwokleung, 2007](#)). Based on this concept, some researchers have put effort into robust designs of various kinds of structural systems under different uncertainties

(Doltsinis and Zhan, 2004; Beer and Liebscher, 2008). In contrast to the design of structures, the geotechnical uncertainty may significantly influence the design associated with geotechnical problems (Phoon and Kulhawy, 1999). Recently, Juang and Wang (2013) proposed a robust geotechnical design (RGD) methodology and applied it to different forms of geotechnical problems such as spread foundations, drilled shafts (Juang et al., 2013) and braced excavations (Juang, et al., 2014). Gong et al. (2014) have applied the robustness design concept for the design of segmental tunnel linings, the idea of this robust design model is to reduce the variation of tunnel lining performance under normal conditions caused by the uncertainty of the input design parameters.

The aim of this paper is to present a general framework for the rehabilitation design for segmental linings from shield tunnelling under the conceptual umbrella of robustness. The goal of robust retrofitting design is to enhance the robustness of the reinforced segmental linings against the design uncertainties with consideration given to minimizing cost, which can be accomplished by varying the design parameters to minimize the variation of the reinforced segmental tunnel lining performance given some uncertainty level of the surrounding environments. The general framework for a robust design model is presented first. Secondly a two-dimensional finite element model is established to simulate the steel-plate-reinforced segmental tunnel lining for the design. The interactions between the steel plates and the lining and also between the lining and the surrounding ground are carefully modelled and verified by full-scale load test results. Finally, a detailed design example is carried out

demonstrating the applicability of proposed robust design methodology for the rehabilitation of segmental tunnel linings using steel plates.

## **2. Framework of robust retrofitting design for segmental tunnel linings**

### **2.1 Practical design method of steel plate strengthening**

Figure 1 presents a photograph showing segmental tunnel linings strengthened by steel plates in the Shanghai metro. The steel plates were installed separately and welded together to form an integral ring. Epoxy was injected into the gap and to provide a bond between the lining and the steel plates. Due to the complexity and potentially large differences between the damaged tunnel conditions from case to case, there isn't a common design method for the steel plate rehabilitation method. In fact, the steel plates are usually only applied to damaged tunnel linings with a horizontal convergence of over 10cm. The size of the steel plates used is nearly the same in each case based on past engineering experience, having a width of 850mm and a thickness of 20~30mm. Although this may be convenient in practice, there is certainly room for improvement and optimization in the design of steel plate reinforcement for particular cases.

### **2.2 Robust retrofitting design methodology**

In the robust rehabilitation design procedure, it is aimed to find an appropriate set of design parameters, which makes the performance of reinforced tunnel lining robust enough with the lowest possible total cost. The horizontal convergence is widely adopted as an indicator of tunnel lining performance both in the research field and in engineering practice (Huang and Zhang, 2016). In this study, the change in



horizontal convergence ( $\Delta D_{hs}$ ) as a result of an environmental impact such as an unexpected ground surface surcharge, compared to the horizontal convergence  $\Delta D_{h0}$  just after the steel plate installation has finished is measured to reflect the performance of segmental tunnel lining reinforced by steel plates. However, the change in the convergence  $\Delta D_{hs}$  as a result of a changed environment will be dependent on multiple sources of uncertainties, for examples the ground properties and the surcharge levels, while the degree of variation in  $\Delta D_{hs}$  can be quantified by its standard deviation to show how sensitive the reinforced segmental tunnel lining is to the noise factors (Juang et al., 2014).

Therefore, the goal of proposed robust retrofitting design is to enhance the robustness of the reinforced segmental tunnel lining against the design uncertainties at low cost, which can be accomplished by varying the design parameters to minimize the standard deviation of the reinforced tunnel performance,  $\Delta D_{hs}$ , given some uncertainty levels of the surrounding environments. As shown in the flowchart in Fig. 3, the robust rehabilitation design procedure is summarized as follows:

Step 1: The problem should initially be defined, with the input parameters being divided into two categories, namely the design parameters (*easy to control* factors) and the *noise* factors (*hard to control* factors) (Kwokleung, 2007). The sizes of the steel plates, such as width ( $w_s$ ) and thickness ( $t_s$ ) are adopted as the design parameters, as these can be specified by the designers. The *noise* factors are the properties of ground such as soil Young's modulus ( $E$ ) and environmental impacts, such as the ground surface surcharge ( $P$ ) in relation to the long-term service life after

rehabilitation.

Step 2: The uncertainty of the *noise* factors is characterized and the domain of the design parameters is defined. In this study, the uncertainty of these noise factors (i.e.  $E$  &  $P$ ) can be characterized using the data from site investigation information and engineering experience. The domain of the design parameters (i.e.  $w_s$  &  $t_s$ ) is specified by the lower and upper bounds of each design parameters, which can be assigned according to the lining segment dimensions, the limitations of tunnel gauge and engineering experience.

Step 3: However, calculating the deformation of the steel-plate-reinforced segmental tunnel lining cannot be solved analytically given the complex interaction problems, and requires numerical simulations. A particular numerical model is established which can simulate the accurate structural response of segmental tunnel linings reinforced by steel plates given certain values of input parameters. The proposed numerical model will be introduced in detail later.

In reality, the steel plates are often applied to severely over-deformed tunnels. Based on the statistics of accidents that occurred to the Shanghai metro tunnels (Huang and Zhang, 2016), the unexpected extreme surcharge on ground surface is the most serious factor among all the environmental disturbances causing large tunnel deformations. Thus, the surcharge is selected as the external environmental uncertainty. In the robust rehabilitation design, the surcharge is simulated by applying pressure to the ground surface above the tunnel within the numerical model. The whole numerical analysis procedure is as shown in Fig. 4, for simplification purposes,

the steps of the initial geostatic stress equilibrium and tunnelling excavation are not described here, as these have been already finished before this procedure starts. The numerical analysis includes following three steps: (1) The surcharge  $P_0$  is applied and the deformation is recorded before the steel plates are added. The horizontal diameter of the tunnel after this step is denoted as  $D_{h0}$ . The specific value of  $P_0$  is determined according to the real tunnel conditions. That is to say, the activation trigger of steel plate and bond spring elements are different from case to case; (2) The steel plate elements and the bond spring elements between the lining and the steel plates are activated in this step to simulate the retrofitting of steel plates to deformed segmental tunnel linings; (3) The surcharge  $P$  is continuously applied in this step. The horizontal diameter of the tunnel after this step is denoted as  $D_h$ . The change in horizontal convergence of the tunnel after applying the steel plates is then calculated e.g.,  $\Delta D_{hs} = D_h - D_{h0}$ .

Step 4: Based on the proposed numerical model, given the characteristics of the noise factors and specific values for the design parameters, the mean value and standard deviation of the reinforced tunnel performance  $\Delta D_{hs}$  need to be evaluated. Recalling that a smaller variation in performance (i.e. in terms of the standard deviation) indicates a higher robustness. However, deriving the mean and standard deviation of the tunnel performance is quite variable, as the performance function for such a problem is a numerical model without an explicit function. Thus the five-point point estimate method (5-point-PEM) procedure proposed by Zhao and Ono (2000, 2001) is adopted here to estimate the mean and standard deviation of  $\Delta D_{hs}$ .

215 Within the proposed 5-point-PEM, the estimating points are obtained in the  
 216 standard normal space. Therefore the random variables ( $x_i$ ) need to be transformed  
 217 into standard normal variables ( $u_i$ ), which can be easily accomplished by the  
 218 *Rosenblatt* transformation (Hohenbichler and Rackwitz, 1981). As for a single  
 219 variable function  $y=y(x)$  the mean and standard deviation of  $y$  can be calculated as  
 220 follows:

$$221 \quad \mu_y = \sum_{j=1}^m P_j y \left[ T^{-1}(u_j) \right] \quad (1)$$

$$222 \quad \sigma_y = \sqrt{\sum_{j=1}^m P_j \left( y \left[ T^{-1}(u_j) \right] - \mu_y \right)^2} \quad (2)$$

223 Where  $T^{-1}(u_j)$  is the inverse *Rosenblatt* transformation,  $\mu_y$  is the mean value of  $y$ ,  
 224  $\sigma_y$  is the standard deviation of  $y$ . The five estimating points in the standard normal  
 225 space and the corresponding weights are:

$$226 \quad \begin{aligned} u_1 &= 0; P_1 = 8/15 \\ u_2 &= -u_3 = 1.3556262; P_2 = P_3 = 0.2220759 \\ u_4 &= -u_5 = 2.8569700; P_4 = P_5 = 1.12574 \times 10^{-2} \end{aligned} \quad (3)$$

227 For a function of multi variables  $G = G(X)$ , where  $X = x_1, x_2, \dots, x_n$ .

$$228 \quad G_i = G[T^{-1}(U_i)] \quad (4)$$

229 Here  $U_i$  means  $u_i$  is the only random variable with other variables equal to the mean  
 230 values. The mean and standard deviation of  $G$  can be obtained using the following  
 231 equations:

$$232 \quad \mu_G = \sum_{i=1}^n \left( \mu_i - G_\mu \right) + G_\mu \quad (5)$$

$$\sigma_G = \sqrt{\sum_{i=1}^n \sigma_i^2} \quad (6)$$

Where  $G_\mu$  is the function value when all variables equal to their mean values,  $\mu_i$  and  $\sigma_i$  are the mean and standard deviation of  $G_i$ , which can be obtained using Eqns. (1) and (2). In this study, to evaluate the variation of the reinforced tunnel performance caused by multi sources of uncertainties,  $\Delta D_{hs}$  could be represented by  $G$ , and the parameter variable vector  $X$  contains the soil Young's modulus ( $E_s$ ) and the ground surface surcharge ( $P$ ). The mean and standard deviation of  $\Delta D_{hs}$  can be easily calculated by Eqns. (3)-(6). More details of the purposed 5-point-PEM can be found in [Zhao and Ono \(2000\)](#).

Let  $n$  denote the number of noise factors, therefore  $M=4*n+1$  calculations will be required for one set of design parameters using the proposed 5-point-PEM. This repetition can be achieved by running the ABAQUS numerical analysis automatically in the Matlab environment.

Step 5: In this step, the mean value and standard deviations for each of the  $N$  designs in the design space are obtained by repeating the analysis in Step 4.

Step 6: For the purposes of getting the most robust design at low cost, the multi-objective optimization algorithm is carried out to yield the Pareto Front in this step. Thus there are two objectives in the robust rehabilitation design strategy, one is to enhance the robustness of segmental tunnel lining strengthened by steel plates, which can be realized by minimizing the standard deviation of  $\Delta D_{hs}$ , and the other one is to minimize the rehabilitation cost.

### 2.3 Cost evaluation

In this study, the total cost of the rehabilitation ( $C$ ) is made up of two main parts, the cost of the material manufacture ( $C_m$ ) and the cost of the construction and installation ( $C_c$ ), which are calculated by following equations:

$$C = C_m + C_c \quad (7)$$

Where  $C_m$  can be further calculated from:

$$C_m = p_s \times (2\pi R_i \times w_s \times t_s \times \rho_s) \quad (8)$$

Where  $p_s$  is the unit price of the steel;  $R_i$  is the inner radius of segmental tunnel lining;  $w_s$  is the width of the steel plates;  $t_s$  is the thickness of the steel plates;  $\rho_s$  is the density of the steel. The unit price of the steel and the construction fee for one ring have been adopted as 30,000 RMB per kilogram and 50,000 RMB respectively, which are based on prices in Shanghai.

### 2.4 Multi-objective optimization

In step 6 of the robust design procedure, a multi-objective optimization problem is established, as shown in Fig. 5. In this case, the constraints contain the lower and upper bounds of each design parameter. In addition, the safety requirement is also implemented as a constraint by insuring the safety factors  $f_s$  above a certain level. In this case, the safety factor  $f_s$  ensuring the safety of the segmental tunnel lining reinforced by steel plates is calculated deterministically using equation:

$$f_s = \frac{\Delta D_{\max}}{\Delta D_{hs,mean}} \quad (8)$$

Where  $\Delta D_{hs,mean}$  is the mean value of the change in horizontal convergence calculated

with all the noise factors being adopted as their mean values.  $\Delta D_{max}$  denotes the maximum transverse convergence deformation of tunnel lining strengthened by steel plates when the bonding failure occurs, i.e. in this case the value is taken as 26mm as observed in the full-scale test carried out by Zhao et al. (2015). Thus a desired safety level could be ensured by giving a specific limit to the safety factors ( $f_{sl}$ ).

With the confirmed design objectives and constraints, the multi-objective optimization algorithm was performed to seek the optimal design solutions. In the general concept of multi-objective optimization, a set of non-dominated solutions, so called the Pareto Front, is obtained rather than a unique solution optimizing all the objectives. Within the set on the Pareto Front, none of them is better than any other with respect to all the objectives, while the designs in this set are superior to all others in the whole design space. That means, each design in the set on the Pareto Front is optimal, as no improvement could be accomplished in one objective without worsening any other objectives (Gong et al., 2014). In this study, the optimal solutions are obtained by using the Non-dominated Sorting Genetic Algorithm version II (NSGA- II) (Deb et al., 2002). The Pareto Front obtained from this process provides a trade-off relationship between the robustness of the reinforced segmental tunnel lining and the rehabilitation cost. The final design depends on the individual situation, for example if a desired robustness is required, the most economical design could be selected from the Pareto Front. Similarly, if the rehabilitation cost needs to be controlled, the design with the highest robustness level at the given cost limit could be obtained. Furthermore, if there is no specific requirement about the robustness and

financial cost, the concept of a knee point may provide the preferred or suggested design within the Pareto Front, which will be explicitly illustrated latter.

### **3. Numerical modeling**

A rational robust design for rehabilitation by using bonding steel plates to shield tunnel lining, as introduced previously, requires a well-established numerical model as a key step in the flowchart. To this end, a two-dimensional finite element model is proposed in this paper for its merit of considering the uncertain soil behaviour and the complex interactions between soils and also between lining and steel plates. The surrounding soil, the tunnel lining, the steel plates and the interactions between each of those are all properly simulated in this model and verified by full-scale test results described in the following sections.

#### **3.1 Establishment of model**

A typical two-dimensional finite element model is established using the commercial finite element code ABAQUS as shown in Fig.5. In this model, the tunnel has an outer diameter  $D_{out}$  of 6.2m. The mesh size of the entire ground model has a width of 100m and a depth of 50m. The selected mesh width is about 16 times the outer diameter which avoids the effect from the boundary on the calculations (Ding et al., 2004), and the mesh utilizes 4710 elements. The soil is simulated using a linear elastic perfectly-plastic model with a Mohr-Coulomb failure criterion. It is noted that there are a number of soil models that more precisely represent the nonlinear behaviour of soils. However, it could be always argued that the elastic perfectly-plastic soil model with a Mohr-Coulomb yield criteria is probably still the



most widely used in numerical simulations, in particular when there are uncertain soil conditions (Mollon et al., 2011; Do et al., 2013). For the Mohr-Coulomb model, the most critical parameters are soil Young's modulus  $E_s$ , Poisson ratio  $\nu$ , soil friction angle  $\varphi$  and cohesion  $c$ . The evaluation of these soil parameters is based on the site investigation report. Table 1 shows the magnitude of these parameters used in this analysis. The interaction between the tunnel extrados and the surrounding soils is simulated using the surface-to-surface contact module in ABAQUS.

Details of the simulation used for the steel plate strengthened segmental lining is shown in Fig.7. The lining segments and the steel plates are simulated as different parts, and assembled together in the calculation, as shown in Fig.7 (a). The behaviour of the concrete lining and the steel plates are assumed to be linear elastic perfectly plastic. The properties are given in Table 2. The tunnel segments are modeled using 4-node bilinear elements and the steel plates are modeled using linear planar beam elements. It should be noted that the width and thickness of the steel plates, being *easy to control* factors in the robust design procedure, could be modified by changing the cross section geometry as an input for the beam elements.

Fig. 7 (b) shows details of the radial joint in the numerical model. A surface-to-surface contact is assigned to the interface between the segments, with the coefficient of friction ratio taken as 0.5 (Liu et al., 2014) and the normal behaviour is a hard contact allowing separation. The tensile and shear characteristics of the joints are represented by a tangential spring ( $k_{j_\theta}$ ) and a radial spring ( $k_{j_r}$ ). The tangential spring ( $k_{j_\theta}$ ) is assigned force-deformation relationship as shown in Fig.8 to simulate

the nonlinear behaviour of two grade 5.8 straight bolts with diameter of 30mm and length of 400mm at the longitudinal joint. The stiffness of the radial spring ( $k_{j_r}$ ) is adopted as  $5 \times 10^8 \text{ N/m}$  (Ding et al., 2004). Hence, the mechanical and deformational behaviour of the longitudinal joint in the tangential, radial and rotational directions could be simulated.

Zhao (2015) proposed a numerical model based on the beam-spring model to investigate the nonlinear response of a segmental lining strengthened by epoxy bonded steel plates. Following their suggestion, the model to simulate the bond behaviour between steel plates and lining incorporates the spring element with normal and shear stiffness, as shown in Fig. 7 (c). The springs allow relative displacement between the connecting nodes in the radial and tangential directions. The shear stiffness and normal stiffness are taken as 6.5 MPa/mm and 60 MPa/mm, respectively, according to the research on epoxy bonded interfaces conducted by Adhikary (2002). Thus the specific stiffness values of the spring elements can be determined according to the element numbers of the spring elements between tunnel lining and steel plates. In this study, 360 pairs of spring elements are distributed uniformly between the lining and steel plates. There are two spring elements in each pair, one in the tangential direction ( $k_{b_\theta}$ ) and the other in the radial direction ( $k_{b_r}$ ). The stiffness values of the three kinds of linear spring elements,  $k_{j_r}$ ,  $k_{b_\theta}$  and  $k_{b_r}$  respectively, can be found in Table 3.

### 3.2 Model validation

The proposed numerical model with the simplifications of the radial joints and

bond behaviour between the lining and steel plates needed be validated either via field data from real case study or from a controlled load test before it could be incorporated into the robust design procedure. Due to the limited number of well-documented case studies, a full-scale test carried out by Zhao et al. (2015) is used in this paper. The test results in terms of tunnel convergence subjected to specific load levels are extracted for validation.

Since the full-scale load test carried out by Zhao et al (2015) is a purely structural test, the soil continuum in the numerical model is not included in this validation. However, the main simplification in the numerical model is the application of the spring element both for the radial joints and the bonding behaviour between the lining and steel plates. Hence, numerically modelling the load structural test was considered sufficient to validate the rationality for the above assumptions.

The test was based on a typical Shanghai metro segmental tunnel lining with 15m overburden of soil, the dimension of which was same with that shown in Fig.2. As shown in Fig. 9, 24 point loads were applied to the external surface of the tunnel lining, which were divided into three groups with different values, P1 (6 loading points), P2 (10 loading points), and P3 (8 loading points). The relative displacement between the top and bottom of the tunnel lining ( $\Delta D_v = D_v - D_v'$ ), i.e. called the vertical convergence, was adopted herein as the indicator of overall deformational response of segmental tunnel linings. As illustrated in Fig. 10, there are three steps for the whole loading process: (1)  $P_2 = P_1 \times 0.65$ ,  $P_3 = 0.5 \times (P_1 + P_2)$ , loaded until P2 equals to the passive earth pressure 275kN; (2)  $P_2 = 275\text{kN}$ ,  $P_3 = 0.5 \times (P_1 + P_2)$ , loading continued

until  $\Delta D_v$  is approximately 120mm, the steel plate beam elements and bond spring elements are active at this point to simulated the application of the steel plates; (3)  $P_2=275\text{kN}$ ,  $P_3=0.5 \times (P_1+P_2)$ , loading then continued until  $P_1=600\text{kN}$ . In the numerical simulations, the load steps and the size of the tunnel lining and steel plates are the same as those used in the test. Further details can be found in [Zhao et al. \(2015\)](#).

The calculated deformational responses from the numerical model were extracted and compared to the experimental results. Fig.10 illustrates the vertical convergence ( $\Delta D_v$ ) against  $P_1$  from both the full-scale test (dotted line) and the numerical analysis (solid line). The deformation of the segmental lining at two stages, i.e. the initial earth pressure loading and the loading after the bonding of the steel plates are both captured by the loading test and numerical analysis. In the first stage, it is observed from the physical and numerical results that the tunnel deformed nonlinearly with an increase in the surrounding load. Obviously, this is due to the nonlinearity of the joints springs and the geometric nonlinearity of the assembled segmental linings. A maximum difference in  $P_1$  between the full-scale test and the numerical analysis is approximately 4.8%, which indicates good agreement even for the largest discrepancy. In the next stage, the deformed segmental linings is reinforced by the steel plates. At this stage the load  $P_1$  is shared by both the lining and the steel plates together. An immediately inflection appears right after the reinforcement, as shown in Fig.11, which proves a significant improvement in the stiffness of the segmental lining due to steel plate reinforcement. A maximum difference of 2.9% is observed between the two

results when  $P_1$  reaches 580kN. However, it should be noted that the failure of segmental lining reinforced by epoxy bonded steel plates cannot be captured by the proposed numerical model since the bonding springs behave linearly. Although, since there is a good agreement between the two results, it was proposed the numerical model could be used for the subsequent deformation analysis of the segmental lining strengthened by bonded steel plates.

#### **4. Application of robust retrofitting design to a case study**

##### **4.1 Case study information**

To illustrate the proposed robust retrofitting design methodology, a repair project of an operational shield tunnel disrupted by an extreme surcharge on the ground surface is introduced, and the proposed robust design methodology is applied to the design for steel plate rehabilitation in this case. As reported by [Huang and Zhang \(2016\)](#), and as shown in Fig.12, a large amount of soil was found to be deposited on the ground surface without permission along the alignment of tunnel of the east extension line of the Shanghai metro line 2. The tunnel had been driven through layers consisting typical Shanghai soft clays, i.e. muddy and silty clays. The cross section of the tunnel is the same as that shown in Fig.1, and the longitudinal joints of the segmental lining were arranged in straight lines. The cover depth of this tunnel is 15~20m. The deposited soil had a height ranging from 2m to 7m creating a large surcharge on the ground surface. The segmental tunnel lining underneath this load area was badly damaged, with a large number of defects, such as lining deformation, cracks and water leakage being detected and threatening the safety of the metro

operation. Details of the geological conditions and the tunnel information can be found in [Huang et al. \(2017\)](#).

As for the emergency response to this accident, a series of rehabilitation methods were applied in the repair work of the damaged tunnel. The lining segment rings from No.500 to No.600 were reinforced using epoxy bonded steel plates. The steel plates had a width of 850mm and thickness of 30mm and were chosen in this case based on practical experience.

## **4.2 Parameters**

The robust design methodology has been subsequently applied to the design of the steel plate rehabilitation for the damaged segmental lined tunnel in this case. The parameters to be used within the numerical model for the proposed design methodology needed to be determined. The properties of the segmental tunnel lining are shown in Table 1. The ground was simplified to homogenous and the geotechnical parameters of the soil were adopted based on the site conditions. As introduced previously, an elastic perfectly plastic constitutive model with a Mohr-Coulomb failure criteria were assigned to the ground soil within the proposed numerical model, with the soil stiffness being indicated by Young's modulus ( $E_s$ ) while the soil strength was given by friction angle ( $\varphi$ ) and cohesion ( $c$ ). Since the variance in the stiffness parameters was more influential than the strength parameters to the tunnel lining deformation, which was of more interest for the robustness analysis, the friction angle ( $\varphi$ ) and cohesion ( $c$ ) were adopted as deterministic values according to the site investigation given by [Huang et al. \(2017\)](#), while the Young's

modulus ( $E_s$ ) was treated as a random variable following lognormal distribution with a mean of 20MPa and a coefficient of variance ( $COV$ ) of 0.3.

The height of the deposited soil within the surcharged area was on average 5m, and assuming that the unit weight of the deposited soil was  $20\text{kN/m}^3$ , the value of the surcharge before reinforcement ( $P_0$ ) was taken as 100kPa. In this case, the surcharge after reinforcement ( $P$ ) was treated as a random variable following a lognormal distribution with a mean of 50kPa and a  $COV$  of 0.4, although it should be noted that the characteristic value of  $P$  will be different from case to case and should be determined according to the design requirements.

As introduced previously, the width  $w_s$  and thickness  $t_s$  of the reinforcing steel plates are design parameters. Considering the manufacturing convenience of steel plates and engineering experience, the range of  $w_s$  was taken from 700mm to 1200mm in increments of 50mm and the range of  $t_s$  was taken from 5mm to 30mm in increments of 2.5mm. As for the cost evaluation of steel plate rehabilitation, the construction fee of steel plate rehabilitation for one ring  $C_c$  was adopted as 50,000 RMB, and the unit price of the steel  $p_s$  was adopted as 30,000 RMB/t in this case. As for the safety requirement, the ultimate horizontal convergence of the reinforced segmental lining was adopted as  $\Delta D_{max}$ , the safety factor ( $f_s$ ) was limited to be higher than 1.5 to ensure the safety of segmental tunnel linings reinforced with bonded steel plates in the future.

### 4.3 Parametric analysis

Before conducting the robust design for the rehabilitation of segmental tunnel

lining using steel plates, a parametric analysis was conducted to investigate the influence of the noise factors ( $E_s$  and  $P$ ) and the design parameters ( $w_s$  and  $t_s$ ) on the design objectives.

In order to illustrate the influence of the soil properties and surcharge value on the segmental tunnel lining performance, the curves of horizontal convergence against surcharge value of tunnel under different conditions are presented in Fig. 13. Comparing the curves for the steel plate reinforced segmental tunnel lining and the one without any treatment, the stiffness is significantly improved due to the reinforcement. For the curves where the soil Young's modulus was taken as mean  $E_\mu$ , the gradient of curve changes from 1.208 to 6.923, which indicates the stiffness of the reinforced tunnel is 5.7 times higher than that of the tunnel without reinforcement. Moreover, by comparing the curves for all the soil Young's modulus values, i.e.  $E_{\mu-\sigma}$ ,  $E_\mu$  and  $E_{\mu+\sigma}$ , it is obvious that the variance in this soil property has an impact on the horizontal convergence. Nevertheless the degree of variation is significantly reduced due to the steel plates, which means the robustness of the segmental tunnel lining could be enhanced to a large degree by bonding steel plates to it.

For the purposes of showing how the design parameters influence the robustness and cost of segmental tunnel lining reinforced by steel plates, the relationship between sizes of steel plates and design cost and robustness are presented in Fig. 14. It is evident that the standard deviation decreases with increase in the steel plate width ( $w_s$ ) or thickness ( $t_s$ ). In addition, comparing the design with  $w_s=1000\text{mm}$  and  $t_s=20\text{mm}$  in Fig.14 (a) and the design with  $w_s=800\text{mm}$  and  $t_s=25\text{mm}$  in Fig.14 (b), the calculated



costs of the steel plate rehabilitation are both 131,340 RMB, while the standard deviation (std) of  $\Delta D_{hs}$  are 1.864 and 1.816 respectively. The cost of the two designs are the same, however the latter one shows a higher level of robustness. This means that the increase in investment could bring about a higher level of robustness, however, the robustness may sometimes be different even with for same cost. Therefore, the optimization shows its importance within the robust design procedure.

#### 4.4 Robust retrofitting design

In this example of the robust retrofitting design procedure, the elastic modulus of soil ( $E_s$ ) and the surcharge after reinforcement ( $P$ ) are the noise factors, while height ( $w_s$ ) and thickness ( $t_s$ ) of reinforcing steel plates are the design parameters. From the parameters introduced previously, the design constraints can be confirmed to include the lower and upper bound of the design parameters and the safety requirement. One of the design objectives is to maximize the design robustness by minimizing the standard deviation of  $\Delta D_{hs}$ , however, the other one is to minimizing the cost of the steel plate rehabilitation. Thus the process of the robust design for rehabilitation of segmental tunnel linings using steel plates is carried out as a multi-objective optimization problem as illustrated in Fig. 15. The Non-dominated Sorting Genetic Algorithm version II (*NSGA-II*) (Deb et al., 2002) has been employed to obtain the Pareto Front for the established multi-objective model.

As shown in Fig. 16, the Pareto Front obtained using *NSGA-II* is marked as hollow circles within the two-dimensional coordinates, where two objectives, the standard deviation of  $\Delta D_{hs}$  and cost, are in x and y axes respectively. Within the

obtained Pareto Front, it is obvious that the robustness tends to increase as the total cost increases, which means that increasing the investment can significantly improve the design robustness. Between all these designs on the Pareto Front, none of them is better than any other in all the objectives, which offers a trade-off relationship between two objectives of robustness and cost. It should be noted that, all the designs on the Pareto Front satisfy the safety requirement.

The obtained designs in the existing Pareto Front are such that a choice of the most optimal single design is not straightforward. Thus engineers need make decision with the help of the trade-off relationship between design robustness and cost. However, the most preferred or recommended design named the ‘knee point’ can be obtained in such a bi-objective problem by using a multi-criteria decision making methodology (Kalyanmoy and Shivam, 2011). A knee point is almost the most preferred design, since a small improvement in any one objective requires an unfavorably large sacrifice in another. The normal boundary intersection method has been adopted herein to locate the knee point on the obtained Pareto Front (Das 1999; Juang et al., 2014). In this method, as shown in Fig. 16, two extreme points  $A$  and  $B$  are obtained to construct the boundary line  $L(A,B)$ . Subsequently, for each design point on the Pareto Front, the distance from the boundary line  $L(A,B)$  can be calculated. Thereafter, the design point with the maximum distance from the boundary line  $L(A,B)$  is defined as the knee point. In this example, the knee point has the following parameters:  $w_s=750\text{mm}$ ,  $t_s=15\text{mm}$  with a cost of  $9.575\times 10^4$  RMB. Above this level, a small improvement in robustness may need a large involvement. While

below this level, a slight cost decrease will significantly reduce the design robustness.

In Fig. 17, design 1 represents the actual design in this case, designs 2 and 3 are the two design point within the obtained Pareto Front, and design 4 is the design yielded by using concept of the knee point. A comparison of these four designs is shown in Table 4. Compared with design 1, the robustness of design 2 is enhanced with little increase in cost, while design 3 yields almost the same robustness with a lower cost. Although the robustness of design 4 is lower than that of design 1, the cost saving is large. Therefore, the significance of the robust retrofitting design proposed in this paper is that the design can be carried out considering both the highest robustness and the lowest cost simultaneously.

## **5. Conclusion**

This paper has presented a general framework for the robust retrofitting design methodology of segmental lined tunnel of shield tunnels using steel plates. The goal of the proposed design methodology is to enhance the robustness of the reinforced segmental tunnel lining against the design uncertainties with respect to achieving low cost, which can be accomplished by varying the design parameters to minimize the variation of the reinforced tunnel performance given some uncertain level in surrounding environments. Specifically, the bonding of steel plates to the lining is selected as a typical example of such a kind of rehabilitation design discussed in this paper. The general framework of the robust design method is initially presented. Then a two-dimensional finite element model is established to simulate the steel plates retrofitting for deformed segmental tunnel linings. The interactions between the steel

plates and the lining and also between the lining and the ground soil are carefully modelled and verified by the full-scale load test results. Finally, a detailed design example is carried out for the applicability of the purposed robust design methodology for rehabilitation of segmental tunnel linings by using steel plates. The results presented in this paper demonstrate the significant potential of utilizing the robust retrofitting design methodology combined with the multi-objective optimization technique where decisions involve different design options and cost. The following conclusions can be draw:

(1) The proposed numerical model was able to simulate the steel plate reinforcement procedure and the structural response of segmental tunnel linings. The deformation of the segmental linings develops nonlinearly with an increase in surcharge loading on the ground surface. The overall stiffness of the segmental lining can be significantly improved due to the installation of steel plates. The uncertainties existing in the surrounding environment, e.g. the soil conditions and the ground surface surcharge, may cause a variation in the performance of the reinforced segmental tunnel lining.

(2) The concept of the robust retrofitting design methodology is introduced in this article, where in this case the design is considered to be robust if the reinforced tunnel performance is insensitive to the variation in the noise factors (in this case, the soil conditions and ground surcharge). The proposed design method is accomplished by varying the design parameters to minimize the standard deviation of reinforced tunnel performance and the cost simultaneously using a multi-objective optimization algorithm.

(3) The Pareto Front derived from the multi-objective optimization reveals trade-off relationships between the design robustness and the rehabilitation cost. Comparing all the designs within the obtained Pareto Front, none is better than any other in achieving all the objectives, and the engineer can make decisions with respect to their own financial restraints or robustness goals. Nevertheless, the most preferred or recommended design could be pointed out with the concept of the knee point.

It should be noted that the robust retrofitting design methodology presented in this paper is a potentially powerful tool that can be applied not only for tunnel linings, but also for other underground or above ground structures. However, the details may be different from case to case. For example, the standard deviation of the tunnel transverse deformation is adopted to indicate the sensitivity to the noise factors in this paper, while the appropriate sensitivity index needs to be selected for a different problem. In addition, in this paper the retrofitting cost is calculated according to the volume of reinforcing steel plate. However, the evaluation of the retrofitting cost may be more precisely represented in other situations by considering the influence of, for example, time. Therefore, further investigation needs to be conducted when adopting this method for solving other geotechnical or structural problems.

## **Acknowledgements**

This study is substantially supported by the Natural Science Foundation Committee Program (No. 51538009, 51608380), by Shanghai Rising-Star Program (17QC1400300), by International Research Cooperation Project of Shanghai Science and Technology Committee (No. 15220721600), by the Shanghai Science and

605 Technology Committee Program (No. 17DZ1204205) and by Peak Discipline  
606 Construction on Civil Engineering of Shanghai Project. Hereby, the authors are  
607 grateful to these programs.

608

609 **Reference:**

- 610 Abaqus. Abaqus User's Manual, Version 6.10. Dassault Systèmes, 2010
- 611 Adhikary, B. B., & Mutsuyoshi, H., 2002. Numerical simulation of steel-plate strengthened  
612 concrete beam by a non-linear finite element method model. *Construction & Building*  
613 *Materials*, 16(5), 291-301.
- 614 Beer, M., & Liebscher, M., 2008. Designing robust structures – a nonlinear simulation based  
615 approach. *Computers & Structures*, 86(10), 1102-1122.
- 616 Chang, C. T., Sun, C. W., Duann, S. W., & Hwang, R. N., 2001. Response of a taipei rapid  
617 transit system (trts) tunnel to adjacent excavation. *Tunnelling & Underground Space*  
618 *Technology*, 16(3), 151-158.
- 619 Chang, C. T., Wang, M. J., Chang, C. T., & Sun, C. W., 2001. Repair of displaced shield  
620 tunnel of the taipei rapid transit system. *Tunnelling & Underground Space Technology*,  
621 16(3), 167-173.
- 622 Das, I., 1999. On characterizing the “knee” of the pareto curve based on normal-boundary  
623 intersection. *Structural Optimization*, 18(2-3), 107-115.
- 624 Deb, K., Pratap, A., Agarwal, S., & Meyarivan, T., 2002. A fast and elitist multiobjective  
625 genetic algorithm: nsga-ii. *IEEE Transactions on Evolutionary Computation*, 6(2),  
626 182-197.
- 627 Ding, W. Q., Yue, Z. Q., Tham, L. G., Zhu, H. H., Lee, C. F., & Hashimoto, T., 2004. Analysis  
628 of shield tunnel. *International Journal for Numerical & Analytical Methods in*  
629 *Geomechanics*, 28(1), 57-91.
- 630 Doltsinis, I., & Zhan, K., 2004. Robust design of structures using optimization methods.  
631 *Computer Methods in Applied Mechanics & Engineering*, 193(23–26), 2221-2237.
- 632 DGJ08-11, 2010. Shanghai foundation design code (DGJ08-11-2010). Shanghai: Shanghai  
633 Construction Committee. (in Chinese).
- 634 Do, N. A., Dias, D., Oreste, P., & Djeran-Maigre, I., 2013. 2D numerical investigation of  
635 segmental tunnel lining behavior. *Tunnelling & Underground Space Technology*, 37(6),  
636 115-127.
- 637 Do, N. A., Dias, D., Oreste, P., & Djeran - Maigre, I. 2015. A new numerical approach to the  
638 hyperstatic reaction method for segmental tunnel linings. *International Journal for*  
639 *Numerical & Analytical Methods in Geomechanics*, 38(15), 1617-1632.
- 640 Gong, W., Wang, L., Juang, C. H., Zhang, J., & Huang, H., 2014. Robust geotechnical design

641 of shield-driven tunnels. *Computers & Geotechnics*, 56(1), 191-201.

642 Gong, W., Huang, H., Juang, C. H., Atamturktur, S., & Brownlow, A., 2014. Improved shield  
643 tunnel design methodology incorporating design robustness. *Canadian Geotechnical*  
644 *Journal*, 52(10), 150226181849001.

645 Hohenbichler, M., and Rackwitz, R., 1981. "Non-normal dependent vectors in structural  
646 safety." *J. Engrg. Mech.*, ASCE, 107(6), 1227–1238.

647 Huang, H. W., & Zhang, D. M., 2016. Resilience analysis of shield tunnel lining under  
648 extreme surcharge: characterization and field application. *Tunnelling & Underground*  
649 *Space Technology*, 51, 301-312.

650 Shao, H., Huang, H. W., Zhang, D. M., & Wang, R. L., 2016. Case study on repair work for  
651 excessively deformed shield tunnel under accidental surface surcharge in soft clay.  
652 *Chinese Journal of Geotechnical Engineering*. (in Chinese)

653 Huang, H.W., Shao, H., Zhang, D., & Wang, F., 2017. Deformational responses of operated  
654 shield tunnel to extreme surcharge: a case study. *Structure & Infrastructure Engineering*,  
655 1-16.

656 Juang, C. H., & Wang, L., 2013. Reliability-based robust geotechnical design of spread  
657 foundations using multi-objective genetic algorithm. *Computers & Geotechnics*, 48(4),  
658 96–106.

659 Juang, C. H., Wang, L., Liu, Z., Ravichandran, N., Huang, H., & Zhang, J., 2013. Robust  
660 geotechnical design of drilled shafts in sand: new design perspective. *Journal of*  
661 *Geotechnical & Geoenvironmental Engineering*, 139(12), 2007-2019.

662 Juang, C. H., Wang, L., Hsieh, H. S., & Atamturktur, S., 2014. Robust geotechnical design of  
663 braced excavations in clays. *Structural Safety*, 49, 37-44.

664 Phoon, K. K., & Kulhawy, F. H., 1999. Characterization of geotechnical variability.  
665 *Foundation Engineering in the Face of Uncertainty@Honoring Fred H. Kulhawy* (Vol.36,  
666 pp.612-624). ASCE.

667 Kiriya, K., Kakizaki, M., Takabayashi, T., Hirose, N., Takeuchi, T., & Hajohta, H., et al.,  
668 2005. Structure and construction examples of tunnel reinforcement method using thin steel  
669 panels. *Nippon Steel Technical Report* (92), 45-50.

670 Kasper, T., & Meschke, G., 2006. A numerical study of the effect of soil and grout material  
671 properties and cover depth in shield tunnelling. *Computers & Geotechnics*, 33(4-5),  
672 234-247.

673 Kwokleung Tsui., 2007. An overview of taguchi method and newly developed statistical  
674 methods for robust design. *Iie Transactions*, 24(5), 44-57.



675 Kalyanmoy Deb, & Shivam Gupta., 2011. Understanding knee points in bicriteria problems  
676 and their implications as preferred solution principles. *Engineering Optimization*, 43(11),  
677 1175-1204.

678 Liu, Z., & Zhang, D., 2014. The mechanism and effects of afrp reinforcement for a shield  
679 tunnel in soft soil. *Modern Tunnelling Technology*, 51(5), 155-160.

680 Liu, C., Zhang, Z., & Regueiro, R. A., 2014. Pile and pile group response to tunnelling using a  
681 large diameter slurry shield – case study in shanghai. *Computers & Geotechnics*, 59(59),  
682 21-43.

683 Mollon, G., Dias, D., Soubra, A. H., & Asce, M. 2011. Probabilistic analysis of pressurized  
684 tunnels against face stability using collocation-based stochastic response surface method.  
685 *Journal of Geotechnical & Geoenvironmental Engineering*, 137(4), 385-397.

686 Ministry of Construction of the People's Republic of China (MCPRC). Code for design of  
687 strengthening concrete structure (GB50367-2013). China Building Industry Press; 2013 [in  
688 Chinese].

689 Shi, P., & Li, P., 2015. Mechanism of soft ground tunnel defect generation and functional  
690 degradation. *Tunnelling & Underground Space Technology*, 50, 334-344.

691 Taguchi, G., & Wu, Y. I. (1979). Introduction to off-line quality control system. *Journal of*  
692 *Food Protection*, 51(6), 449-451(3).

693 Yuan, Y., Jiang, X., & Liu, X., 2013. Predictive maintenance of shield tunnels. *Tunnelling &*  
694 *Underground Space Technology*, 38(3), 69–86.

695 Ziraba, Y. N., & Baluch, M. H., 1995. Computational model for reinforced concrete beams  
696 strengthened by epoxy bonded steel plates. *Finite Elements in Analysis & Design*, 20(4),  
697 253-271.

698 Zhao, Y. G., & Ono, T., 2000. New point estimates for probability moments. *Journal of*  
699 *Engineering Mechanics*, 126(4), 433-436.

700 Zhao, Y. G., & Ono, T., 2001. Moment methods for structural reliability. *Structural Safety*,  
701 23(1), 47-75.

702 Zhang, D. M., Zou, W. B., & Yan, J. Y., 2014. Effective control of large transverse  
703 deformation of shield tunnels using grouting in soft deposits. *Chinese Journal of*  
704 *Geotechnical Engineering*, 36(12), 2203-2212.

705 Zhang, D.M, Phoon, K. K., Hu, Q.F., & Huang, H.W., 2017. Nonlinear subgrade reaction  
706 solution for circular tunnel lining design. *Canadian Geotechnical Journal*. DOI:  
707 <https://doi.org/10.1139/cgj-2017-0006> (online).

708 Zhao, H., Liu, X., Bao, Y., Yuan, Y., & Bai, Y., 2015. Simplified nonlinear simulation of

709 shield tunnel lining reinforced by epoxy bonded steel plates. Tunnelling & Underground  
710 Space Technology, 51, 362-371.  
711

712

713

## **Table and Figure Captions**

714 **Tables:**

715 Table 1 Properties of soil

716 Table 2 Parameters for the segmental tunnel concrete lining and steel plates

717 Table 3 The stiffness values of the spring elements simulating the segmental joints

718 and epoxy bonding behaviour

719 Table 4 Comparison between the actual design and the optimal designs derived by the

720 robust retrofitting design methodology

721 **Figures:**

722 Figure 1 Photograph of a steel plates reinforced segmental tunnel lining

723 Figure 2 Diagram of showing an example of segmental tunnel linings reinforced by

724 steel plates

725 Figure 3 Flowchart for developing a robust retrofitting design

726 Figure 4 Numerical analysis procedure

727 Figure 5 Multi-objective optimization formulation for robust retrofitting design

728 Figure 6 Finite element mesh for the ground

729 Figure 7 Finite element model for steel plates reinforced segmental linings, (a) the 2D

730 model for the full reinforced tunnel lining, (b) the radial lining joint, (c) modelling the

731 bond between the steel plates and the lining segment

732 Figure 8 Force-deformation relationship assigned to tangential spring in the segment

733 joint

734 Figure 9 Schematic of the applied loading

735 Figure 10 The loading process for P1, P2 and P3

736 Figure 11 Comparison between the full-scale test results and the numerical analysis

737 results

738 Figure 12 Location of the surcharge area

739 Figure 13 Curves showing the horizontal convergence ( $\Delta D_h$ ) against surcharge value

740 Figure 14 Influence of steel plate size on cost and robustness, (a) influence of steel

741 plate width ( $w_s$ ), (b) influence of steel plate thickness ( $t_s$ )

742 Figure 15 Formulation of the robust design for the rehabilitation of segmental tunnel

743 linings using steel plates

744 Figure 16 Pareto front obtained using NSGA-II

745 Figure 17 Comparison between the actual design and the optimal designs on the

746 Pareto Front

747

748

749

Table 1 Properties of soil ([Huang et al., 2017](#))

Parameters	Symbol	Unit	Value (or mean value)	COV	Distribution
Poisson's ratio	$\nu$	-	0.167	-	-
Unit weight	$\gamma$	kN/m <sup>3</sup>	18	-	-
Cohesion	$c$	kPa	15	-	-
Friction angle	$\varphi$	°	15	-	-
Young's modulus	$E_s$	MPa	20	0.3	Lognormal

750

751

752 Table 2 Parameters for the segmental tunnel concrete lining and steel plates

	Young's modulus /MPa	Poisson's ratio	Yielding stress /MPa
C55 concrete	35.5	0.167	25.3
steel plates	$2 \times 10^5$	0.2	215

753

Table 3 The stiffness values of the spring elements simulating the segmental joints

and epoxy bonding behaviour

Position	Direction	Symbol	stiffness (N/m)
segmental joints	radial	$k_{j_r}$	$5 \times 10^8$
epoxy bonding	tangential	$k_{b_\theta}$	$3.74 \times 10^8$
	radial	$k_{b_r}$	$3.45 \times 10^9$

759

760 Table 4 Comparison between the actual design and the optimal designs derived by the

761 robust retrofitting design methodology

Design Point	$w_s$ /mm	$t_s$ /mm	std of $\Delta D_{hs}$ /mm	Cost / $\times 10^4$
1	850	30	1.800	15.571
2	950	27.5	1.624	15.625
3	750	27.5	1.767	13.388
4	700	17.5	2.324	9.982

762



763



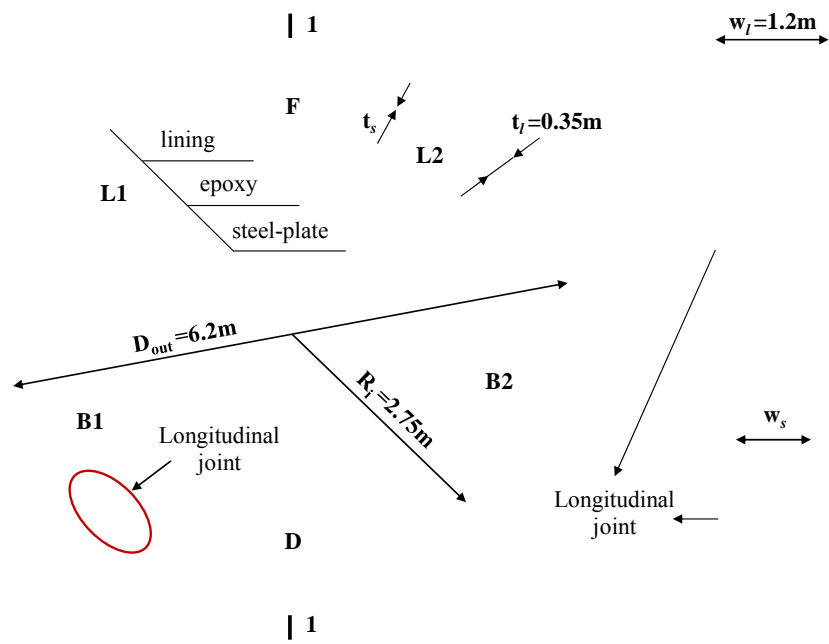
764

765

Figure 1 Photograph of a steel plate reinforced segmental tunnel lining

766

767



768

769 Figure 2 Diagram of showing an example of segmental tunnel linings reinforced by  
 770 steel plates

771

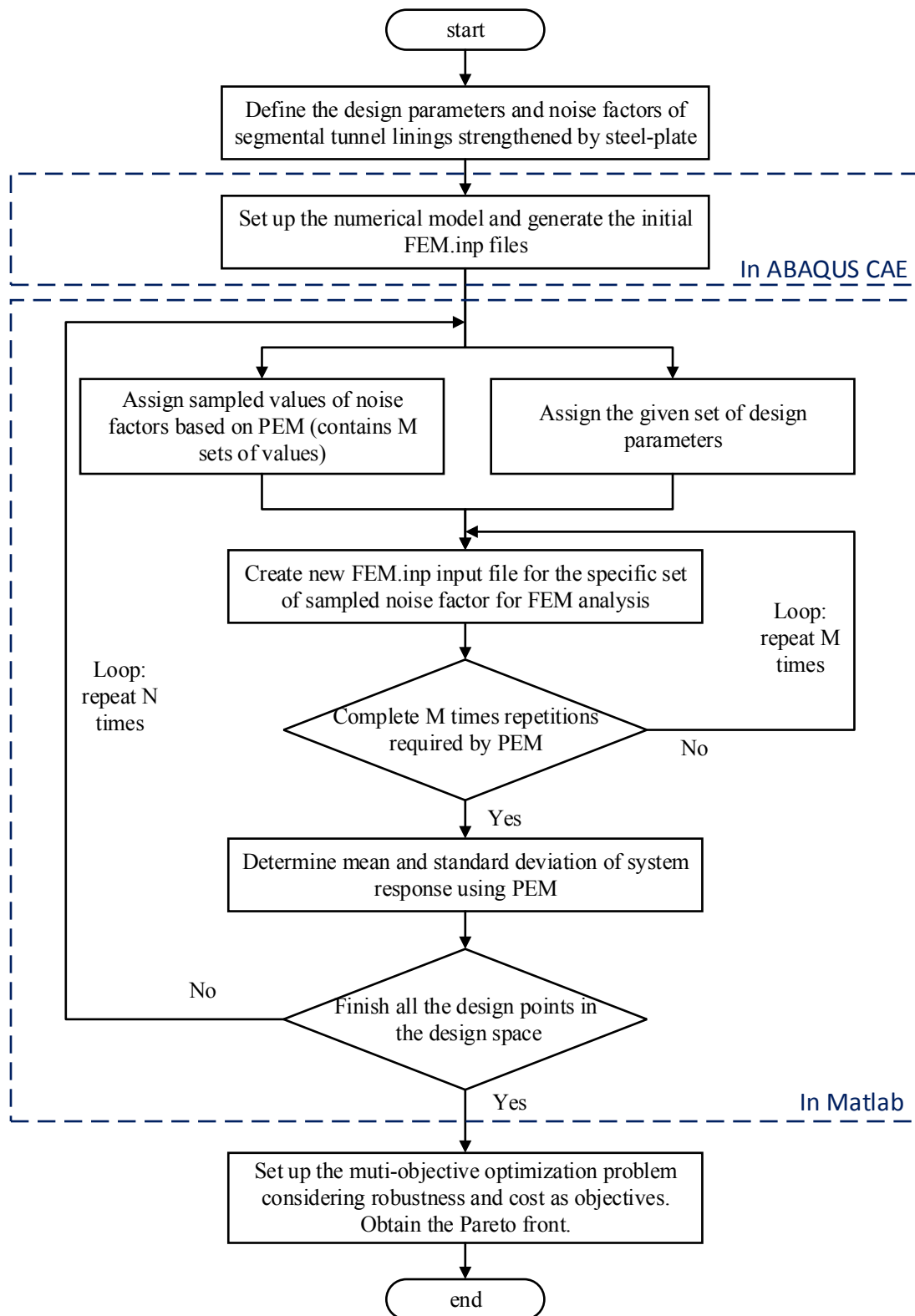
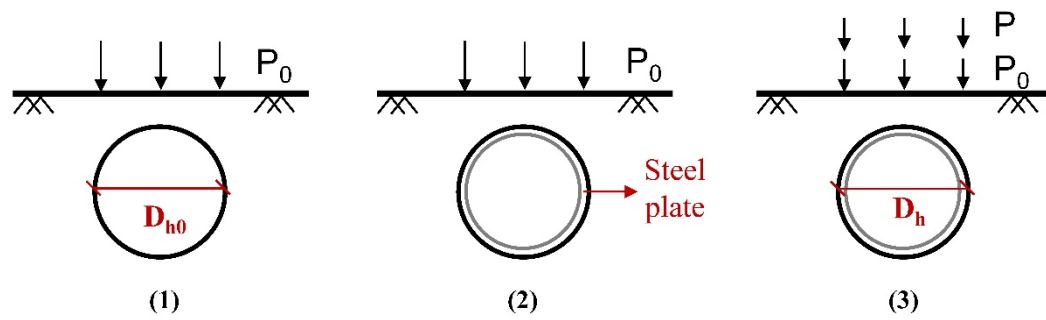


Figure 3 Flowchart for developing a robust retrofitting design

776



777

778

Figure 4 Numerical analysis procedure

779

780

**Find value of design parameters:**  
 $w_s$  (width of reinforcing steel plate)  
 $t_s$  (thickness of reinforcing steel plate)

**Subjected to constraints:**  
 $w_{sl} \leq w_s \leq w_{su}$   
 $t_{sl} \leq t_s \leq t_{su}$   
 $f_s > f_{sl}$

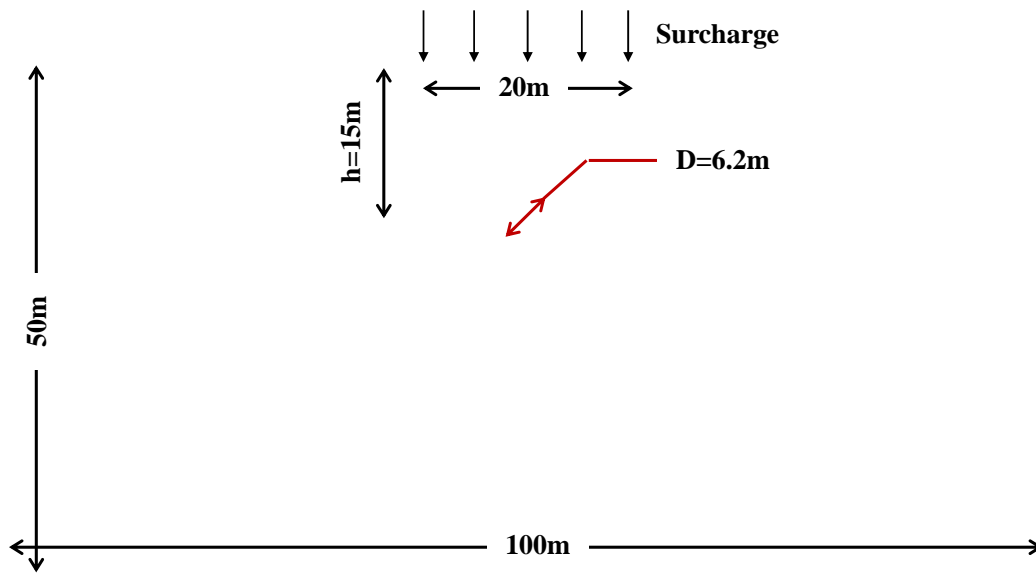
**Objectives:**  
Maximizing the robustness index,  $R_s$   
Minimizing the cost,  $C$

781

782 Figure 5 Multi-objective optimization formulation for robust retrofitting design

783

784



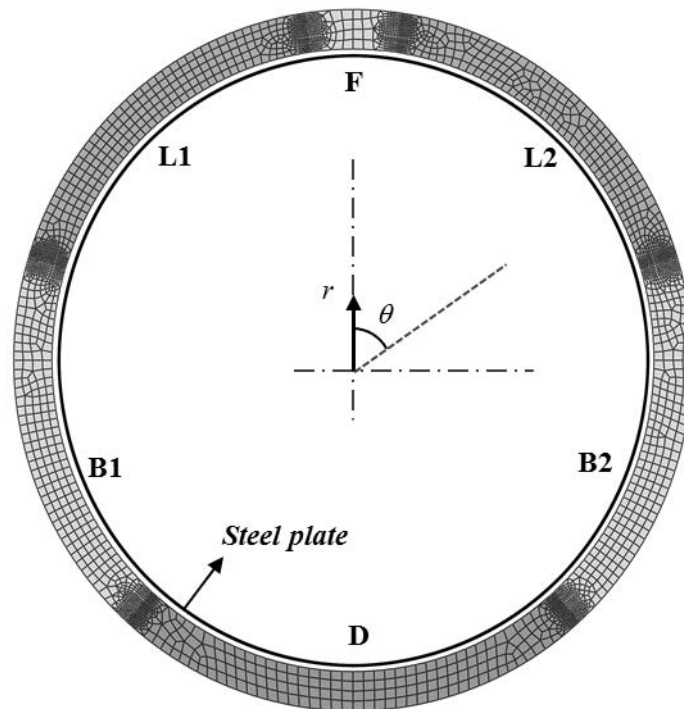
785

786

Figure 6 Finite element mesh for the ground

787

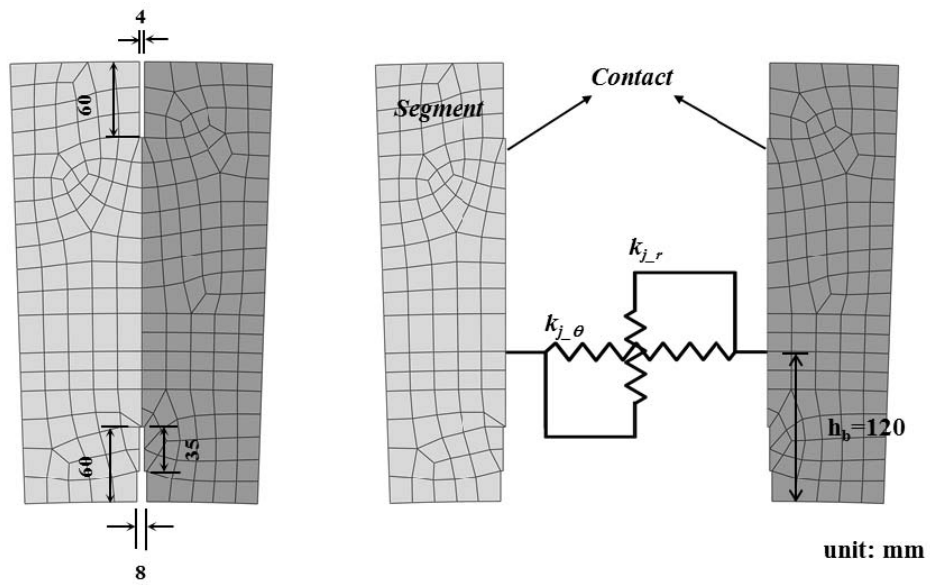
788



789

790

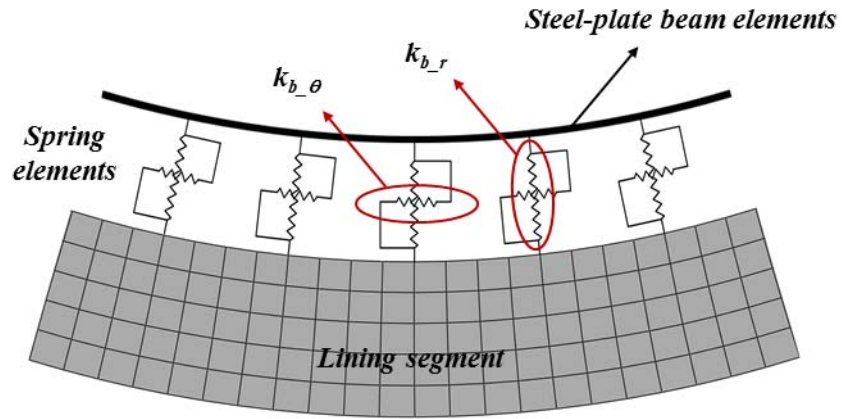
(a)



791

792

(b)

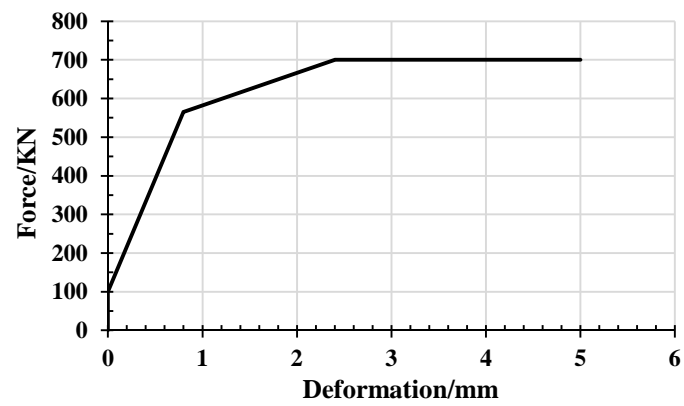


(c)

Figure 7 Finite element model for steel plates reinforced segmental linings, (a) the 2D model for the full reinforced tunnel lining, (b) the radial lining joint, (c) modelling the bond between the steel plates and the lining segment



799



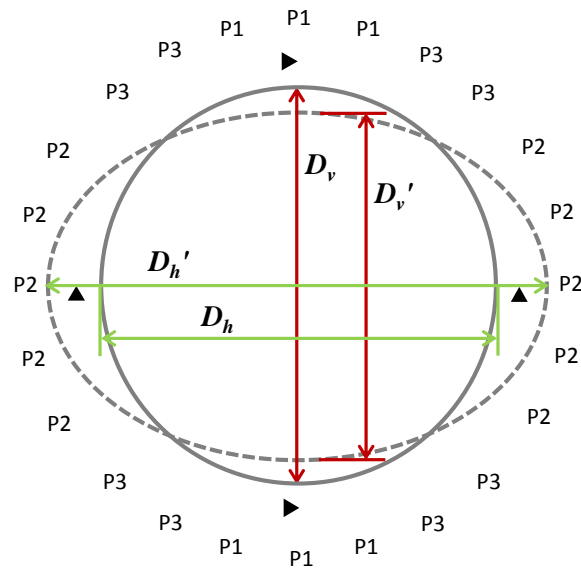
800

801 Figure 8 Force-deformation relationship assigned to tangential spring in the segment

802 joint

803

804



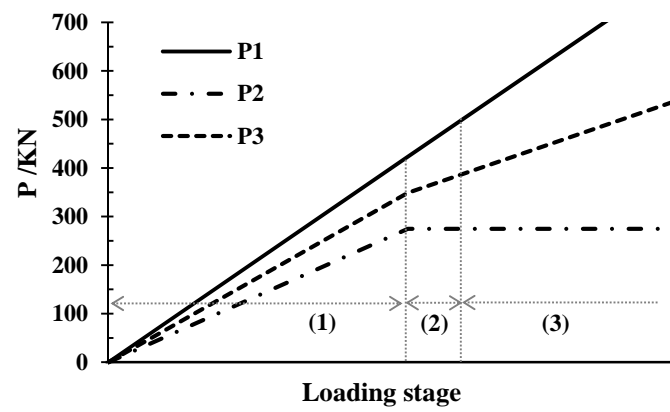
805

806

Figure 9 Schematic of the applied loading

807

808



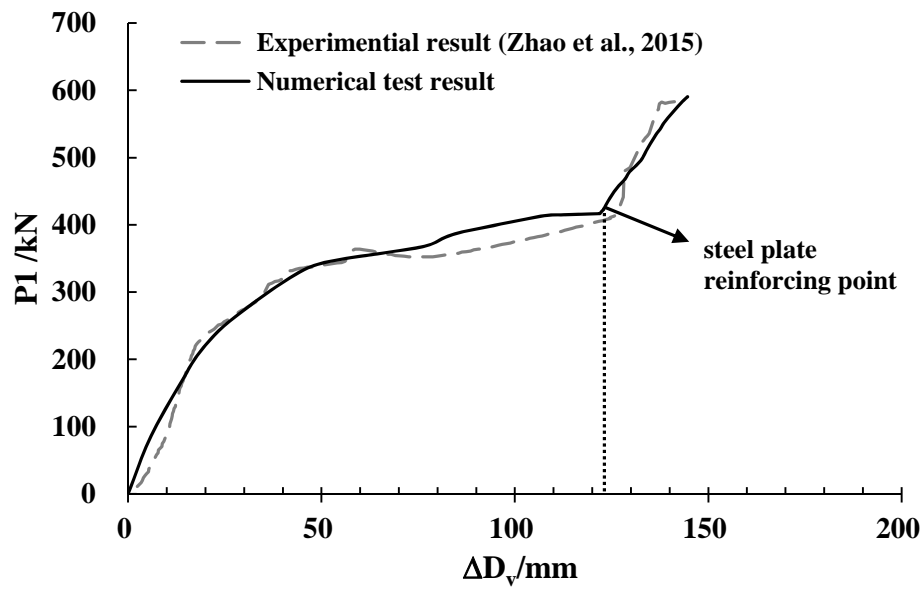
809

810

Figure 10 The loading process for P1, P2 and P3

811

812



813

814 Figure 11 Comparison between the full-scale test results and the numerical analysis

815 results

816

817



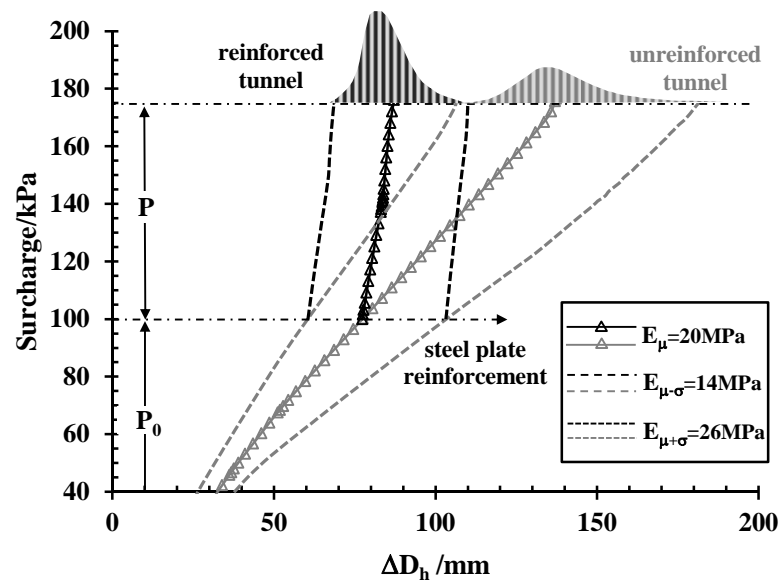
818

819

Figure 12 Location of the surcharge area (Huang et al., 2017)

820

821

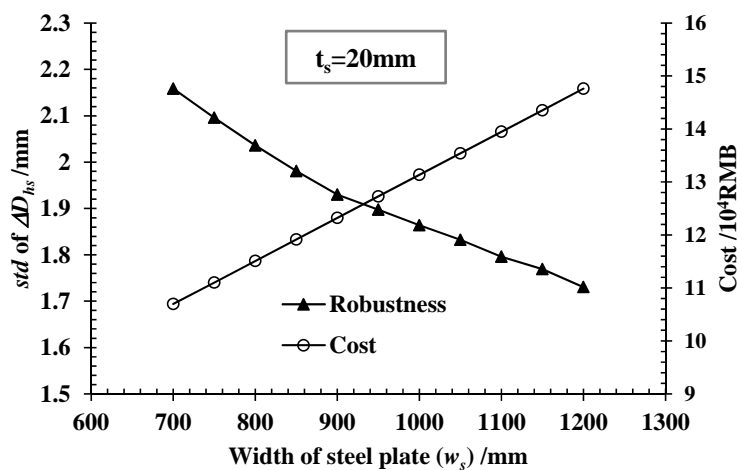


822

823 Figure 13 Curves showing the horizontal convergence ( $\Delta D_h$ ) against surcharge value

824

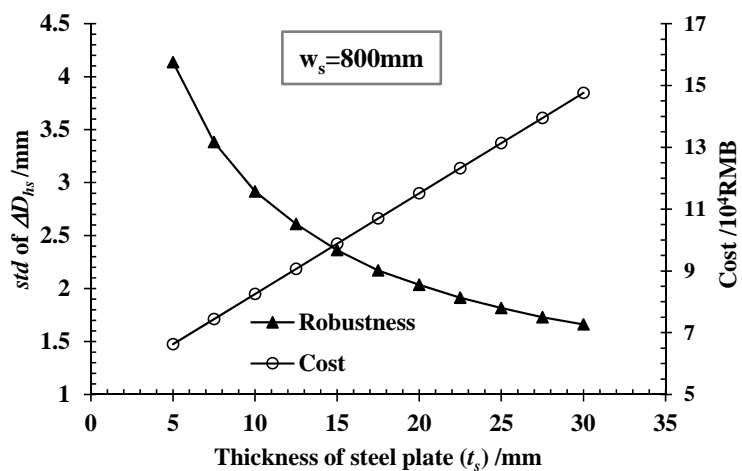
825



826

827

(a)



828

829

(b)

830 Figure 14 Influence of steel plate size on cost and robustness, (a) influence of steel  
831 plate width ( $w_s$ ), (b) influence of steel plate thickness ( $t_s$ )

832

833

**Find value of design parameters:**

$w_s$  (width of reinforcing steel plate)

$t_s$  (thickness of reinforcing steel plate)

*unit:mm*

**Subjected to constraints:**

$700 \leq w_s \leq 1200$  (with interval of 50)

$5 \leq t_s \leq 30$  (with interval of 2.5)

Safety factor  $f_s > 1.5$

**Objectives:**

Minimizing the standard deviation of  $\Delta D_{hs}$  (mm)

Minimizing the cost of steel plate reinforcement (RMB)

834

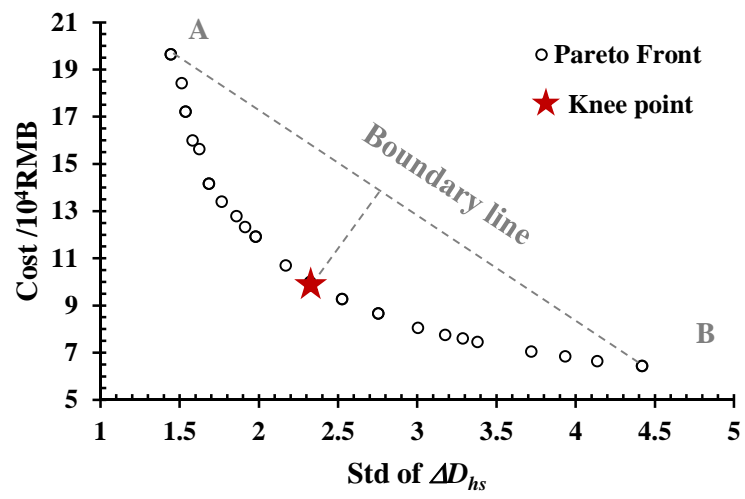
835 Figure 15 Formulation of the robust design for the rehabilitation of segmental tunnel

836 linings using steel plates

837



838



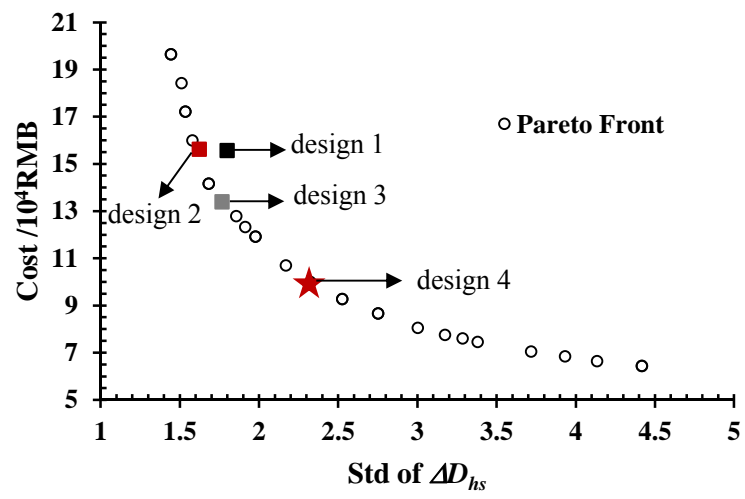
839

840

Figure 16 The Pareto Front obtained using NSGA-II

841

842



843

844 Figure 17 Comparison between the actual design and the optimal designs on the

845 Pareto Front

846